ILASS–Europe 2022, 31th Conference on Liquid Atomization and Spray Systems, 6-8 September 2022, Virtual, Israell

Performing Passive Advection Tests via Analytical Time Step Calculation Using the VOF Method

Jonas Steigerwald*[1], Corine Kieffer-Roth[1], Bernhard Weigand[1]
Institute of Aerospace Thermodynamics (ITLR), University of Stuttgart, Germany
*Corresponding author: jonas.steigerwald@itlr.uni-stuttgart.de

Abstract
Accurate numerical simulations of multiphase flow phenomena like jet breakup or drop film interactions require an accurate advection of the disperse phase. A proper validation of the used numerical advection scheme is therefore of key importance. In order to validate these schemes, it is standard practice to perform advection tests in which simple geometrical objects are passively advected with a given solenoidal velocity field within the computational domain. Test results are then compared with other results from literature. For tests with a temporal varying velocity field, different approaches are used in literature which have in common that the obtained results depend on the used temporal discretization scheme of the multiphase flow solver. In this work, we present a methodology for performing passive advection tests with temporally varying solenoidal velocity fields using the Volume-of-Fluid (VOF) method whose results are independent of the used temporal discretization scheme. In the proposed methodology, the volume fluxes of the advected fluid across the faces of the grid cells are determined with spatial as well as temporal averaged velocities. The time step needed for the temporal integration of the velocity field is calculated analytically by applying the fundamental theorem of calculus to the underlying Courant-Friedrichs-Lewy (CFL) condition, which is therefore exactly fulfilled during the advection. Due to that, test results are independent of the temporal discretization scheme of the used solver and the temporal resolution solely depends on the chosen CFL-number. This promotes the compatibility of test results and can help to prevent a biased view on different test results from the literature in the future. The proposed methodology is exemplarily applied to a two-dimensional flow test often used in literature and its advantages are demonstrated by means of a detailed analysis of the test results.

Keywords
Volume-of-Fluid (VOF) method, Courant-Friedrichs-Lewy (CFL) number, Deformation flow, Passive advection test

Introduction

Passive advection tests have been a widely established and effective way to test the capabilities of interface reconstruction methods and advection schemes of multiphase flow solvers for decades [1-14]. In these tests, simple geometrical objects like circles or spheres are passively advected with a given stationary or temporal varying solenoidal velocity field $\mathbf{u}(\mathbf{x}, t)$ by using a transport equation

$$\frac{\partial \chi(\mathbf{x}, t)}{\partial t} + \nabla \cdot (\chi(\mathbf{x}, t)\mathbf{u}(\mathbf{x}, t)) = 0, \tag{1}$$

where the phase indicator function $\chi(\mathbf{x}, t)$ marks the advected object. A common feature of most test cases is the periodicity through which the translated, rotated or deformed object will reach its initial position again after a specific amount of time. This periodicity enables a comparison between the advected and initialized state of the object, which then provides important insights into the accuracy and the conservativity of the used advection scheme. In

addition, test results can be used to compare different numerical solvers which may be based on different numerical methods.

A popular method for advecting multiple fluids, which are separated by a sharp interface, is the interface-capturing Volume-of-Fluid (VOF) method by Hirt and Nichols [15]. The VOF method introduces the volume fraction of the reference fluid Ω per grid cell

$$f_C(t) = \frac{1}{\Delta V_C}\int_{V_C} \chi(\mathbf{x},t)\,\mathrm{d}V \quad \text{with} \quad \chi(\mathbf{x},t) = \begin{cases} 1 & \text{if } x \in \Omega \text{ at time } t, \\ 0 & \text{else,} \end{cases} \tag{2}$$

as a spatial average of the phase indicator function $\chi(\mathbf{x},t)$, where ΔV_C denotes the volume of a grid cell C. If equation (2) is inserted into equation (1) this yields after discretization, integration over space and time and by applying the divergence theorem

$$f_C^{n+1} - f_C^n = -\frac{1}{\Delta V_C}\sum_{S=1}^{N_S} F_S \qquad \text{with} \quad F_S = \int_t^{t+\Delta t}\int_S \chi(\mathbf{x},t)\mathbf{u}(\mathbf{x},t)\cdot\mathbf{n}\mathrm{d}S\mathrm{d}t\,, \tag{3}$$

where $\mathbf{n}_S$ denotes the unit normal vector of cell face S, N_S is the number of cell faces and $\mathrm{d}S$ is the infinitesimal cell face area. The volume fluxes F_S, which are still exact in the presented form and whose accurate calculation is the basis of every VOF advection scheme, have in general to be approximated with $F_S \approx g_S^n$. The reason for this is that the unknown temporal evolution of the reference fluid Ω prevents the temporal integration of $\chi(\mathbf{x},t)$ over the time interval $[t, t+\Delta t]$. The fluxes are therefore calculated by only using the state of the reference fluid at time t or at the discrete time level t^n, respectively, and by using the velocity field $\mathbf{u}(\mathbf{x},t)$. In case a passive advection test shall be performed, the velocity field $\mathbf{u}(\mathbf{x},t)$ is known. If $\mathbf{u}$ is stationary, the calculation of the fluxes is a simple task since the temporal averaged $\bar{\mathbf{u}} = \mathbf{u}$. If, however, the velocity field is temporally varying, the incorporation of the given velocity field into the solution cycle of the governing advection equation is not trivial since the necessary time step Δt for the temporal integration in equation (3) is unknown. Two common approaches are to set Δt either to a constant value so that Δt satisfies initially the underlying time step constraint (see e.g. [9]), or to calculate Δt adaptively throughout the simulation also by using a time step constraint (see e.g. [11]). In both approaches test results are, however, affected by the used temporal discretization scheme of the used solver which bias the results and thus the comparability between different solvers. Since an accurate and standardized calculation of the volume fluxes is, however, crucial for interpreting and comparing the sensitive results of passive advection tests, we present a methodology in the following how the necessary time step Δt for the temporal integration in equation (3) can be obtained analytically so that test results become independent of the used temporal discretization scheme.

Methodology

The basis of the proposed methodology is the underlying time step constraint whose definition usually depends on the advection scheme as well as on the used grid. Since the focus of this paper is only to demonstrate the methodology, it is exemplarily shown for rectilinear grids. In such a case, the time step constraint is the classical Courant–Friedrichs–Lewy (CFL) condition, which limits the ratio of the advection distance to the size of the corresponding grid cell (i,j,k). If this condition is applied to each dimension separately, how it is done in many numerical solvers, these constraints read for a three-dimensional scenario

$$a \geq \frac{\left|u_{i+1/2,j,k}^n\right|\Delta t_x}{\Delta x_i^+}, \qquad a \geq \frac{\left|v_{i,j+1/2,k}^n\right|\Delta t_y}{\Delta y_j^+}, \qquad a \geq \frac{\left|w_{i,j,k+1/2}^n\right|\Delta t_z}{\Delta z_k^+}, \tag{4a-c}$$

where u, v, w denote the velocity components, a the CFL-number, $\Delta d_\eta^+ = \min(\Delta d_\eta, \Delta d_{\eta+1})$ with dimension $d \in \{x, y, z\}$ and cell index η, and Δt_d the corresponding time steps. The global time step $\Delta t = \min(\Delta t_d)$ for a solution cycle is usually calculated by using the velocity values after the previous time step t^n. This leads, however, to a varying effective CFL-number a in case the velocity changes with time since the numerators in equations (4a-c) are only linear approximations. In contrast to that, the proposed methodology uses spatial as well as temporal averaged cell face velocities for the calculation of g_S^n, as for example

$$\bar{u}_S = \frac{1}{\Delta t A_S} \int_{t^n}^{t^n+\Delta t} \int_S u(x, y, z, t) \cdot \mathbf{n} \mathrm{d}S \mathrm{d}t, \tag{5}$$

where the component u of the fully known velocity field $\mathbf{u}$ is integrated over the corresponding cell face S with area A_S, over the time interval $[t^n, t^n + \Delta t]$ and divided by the intervals of integration. Since we require that the CFL-conditions are always exactly fulfilled independent of the rate of change of the velocity field, the averaged velocity components are inserted into equations (4a-c). The subsequent determination of Δt by using the resulting averaged CFL-conditions is, however, not obvious due to the fact that Δt is multiplied with temporal averaged velocities for which Δt itself is used. In order to overcome this obstacle, Δt is calculated by applying the fundamental theorem of calculus to the advection distances, like for example to $|\bar{u}_{i+1/2,j}^n|\Delta t = s_{x,i+1/2,j}^n(\Delta t)$ (visualized in figure 1), which is treated now as a function of Δt that needs to be determined. This leads to an averaged time step constraint e.g. in x-direction

$$a = \frac{s_{x,i+1/2}(\Delta t)}{\Delta x_i^+} = \frac{|\bar{u}_{i+1/2}^n|\Delta t}{\Delta x_i^+} = \frac{\left|\int_{t^n}^{t^n+\Delta t} \int_{y_{j-1/2}}^{y_{j+1/2}} u(x_{i+1/2}, y, t) \mathrm{d}y \mathrm{d}t\right|}{\Delta y_j \Delta x_i^+}. \tag{6}$$

The third equality is guaranteed by the mean value theorem of integration, since we use only solenoidal velocity fields for a passive advection, whose components are continuous functions on the closed test domain and which are differentiable in the open test domain. Equation (6) can be solved for the desired time step Δt after calculating the definite integral of the velocity component u over the corresponding cell face and the time interval $[t^n, t^n + \Delta t]$. The analytical time step calculation has to be done for all cell faces within the computational domain and the smallest time step is set as the global time step. The corresponding temporal averaged velocities (see equation (5)) needed for the calculation of the approximated f-flux $g_{x,i+1/2,j}^n = \bar{u}_{i+1/2,j}^n \mathrm{Vol}/(|\bar{u}_{i+1/2,j}^n|\Delta t \Delta y_j)$ with the advected Ω-volume Vol (see figure 1) can be calculated afterwards.

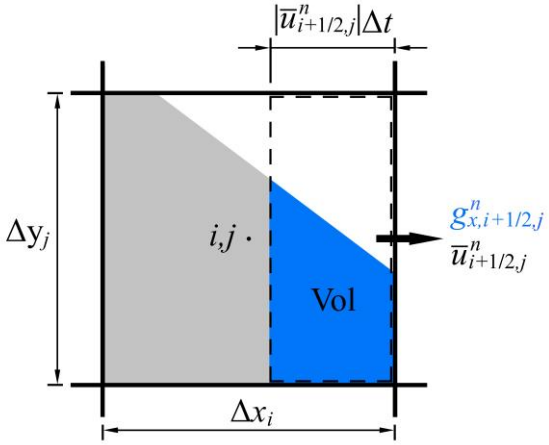

Figure 1. Schematic representation of the f-flux $g_{x,i+1/2,j}^n$ in x-direction through the cell face in case $\bar{u}_{i+1/2,j}^n > 0$.

Numerical Example

In the following, we present the resulting formulae for the analytical timestep calculation using a rectilinear grid for two very often used passive advection tests: The two-dimensional (2D) and three-dimensional (3D) deformation flow by LeVeque [2]. Furthermore, we compare the results of the 2D test with data from the literature, which will demonstrate the sensitivity of the results regarding the incorporation of the averaged velocities into the volume flux calculation.

Setup and numerical implementation

In the advection tests by LeVeque [2], a disk (a sphere in 3D) with a diameter of 0.3 deforms under the influence of a given solenoidal velocity field within a unit square (or cubic) domain and shall reach its initial shape again after the period T. In the 2D case, the disk is initialized at $(0.50, 0.75)$, whereas in the 3D case a sphere is initialized at $(0.35, 0.35, 0.35)$. Since the 3D velocity field is an extension of the 2D velocity field, we present the formulae in the following in a unified manner by introducing the variable r. The variable r specifies the dimensionality of the flow and has to be set to 0 for the 2D case and to 1 for the 3D case. The solenoidal velocity field $\mathbf{u}(\mathbf{x}, t)$ is given by

$$\begin{aligned} u(x,y,z,t) &= 2^r \sin^2(\pi x)\sin(2\pi y)\sin^r(2\pi z)\cos(\pi t/T), \\ v(x,y,z,t) &= -\sin(2\pi x)\sin^2(\pi y)\sin^r(2\pi z)\cos(\pi t/T), \\ w(x,y,z,t) &= -r\sin(2\pi x)\sin(2\pi y)\sin^2(\pi z)\cos(\pi t/T). \end{aligned} \tag{7a-c}$$

The velocity field changes periodically with time due to the LeVeque term $\cos(\pi t/T)$ [4,8].

The first step for determing Δt_{ana} is to calculate the spatial and temporal averaged velocity components $\bar{u}, \bar{v}, \bar{w}$ at each cell face (see exemplarily equation (5)) by integrating equations (7a-c) over the cell face S, which lies in normal direction to the velocity component for the used rectilinear grid, and over the general time interval $[t^n, t^n + \Delta t]$. Next, $\bar{u}, \bar{v}, \bar{w}$ are inserted into the definitions of the CFL-condition (equations (4a-c)). The resulting equations can be solved analytically for the local cell time steps Δt_d, which read[1]

$$\Delta t_d = \frac{T}{\pi}\arcsin(\theta_d) - \tau + \psi\, T, \qquad \tau = t^n - \left\lfloor \frac{t^n}{T} \right\rfloor T, \qquad \psi = \begin{cases} 0 & \text{if } \tau < T/2 \\ 1 & \text{if } \tau \geq T/2 \end{cases} \tag{8a-c}$$

with the $\arcsin$ arguments

$$\theta_x = \frac{2a\pi^{2+r} P_x(i)}{T\,\left|C_y(j)C_z(k)\right|} + (-1)^{\psi}\sin(\pi t/T), \qquad \theta_y = \frac{2^{1+r} a\pi^{2+r} P_y(j)}{T\,|C_x(i)C_z(k)|} + (-1)^{\psi}\sin(\pi t/T),$$

$$\theta_z = \frac{4a\pi^3 P_z(k)}{T\,\left|C_x(i)C_y(j)\right|} + (-1)^{\psi}\sin(\pi t/T) \quad \text{if } r = 1, \tag{9a-c}$$

with

$$C_d(\eta) = \frac{\cos\left(2\pi d_{\eta-1/2}\right) - \cos\left(2\pi d_{\eta+1/2}\right)}{\Delta d_\eta}, \qquad P_d(\eta) = \frac{\Delta d_\eta^+}{\sin^2\left(\pi d_{\eta+1/2}\right)}. \tag{10}$$

The desired global time step Δt_{ana}, which exactly fulfills the global time step contraint, is obtained by taking the minimum of all analytically calculated cell time steps $\Delta t_{ana} = \min(\Delta t_d)$. Finally, the averaged velocities $\bar{u}, \bar{v}, \bar{w}$ needed for the f-fluxes g_S^n can be calculated by using the evaluated Δt_{ana}.

For a proper implementation of the Δt_{ana} calculation, special care has to be taken in situations,

[1] The mathematical operator $\lfloor x \rfloor = \max\{n \in \mathbb{Z} | n < x\}$ denotes the floor function with $x \in \mathbb{R}$.

in which velocities or their derivatives change their sign because the $\arcsin$ arguments θ_d are only specified in the domain $[-1,1]$. There are two possibilities to handle such situations. One possibility is to choose Δt_{ana} in such a way, that $t^{n+1} = T/2$ or an integer multiple of $T/2$, dependent of the current state of the test. In this way, it is not only possible to visualize the advected object exactly at the point in time of its maximum (or minimum) deformation, but also to evaluate the error exactly at $T/2$ or at various integer multiples of $T/2$. Note that this leads to a change of the effective CFL-number a for these specific time steps. The other possibility in the present case is to take advantage of the periodic character of the time dependence of $\mathbf{u}(\mathbf{x}, t)$ (here LeVeque's cosine term). If the velocities or their derivatives change their sign, one can again determine Δt_{ana} in a way, that $t^{n+1} = T/2$ or an integer multiple of $T/2$ and additionally, t^n is set to $t^n_{new} = t^n + 2\Delta t_{ana}$. The calculation of Δt_{ana} has to be repeated afterwards, but now with t^n_{new} instead of t^n. The advantage of this treatment is that the effective CFL-number a remains constant and that the number of solution cycles to perform the test is minimized. However, the state of deformation cannot be analyzed at specific instants in time anymore, which is a fundamental reason for performing passive advection tests.

Results

The implementation is tested with Free Surface (FS3D), a solver originally developed by Rieber [16], with a 3D variant of the split advection scheme by Rider and Kothe [4] (RK3D) and with the interface reconstruction method by Youngs [17]. All tests were performed with the variant which writes out the f-field at $\bar{t} = t/T = 0.5$ and $\bar{t} = 1$ via an additional time step.
Figure 2 shows the reconstructed interface for three Cartesian grids with $N_d = 64$, $N_d = 128$, and $N_d = 256$, where N_d denotes the number of grid cells per dimension d, for $a = 1.0$ and $T = 8$ at the time of maximum disk deformation ($\bar{t} = t/T = 0.5$) and at $\bar{t} = 1$, when the disk should theoretically be in its initial position again. In addition, the results are plotted over a reference solution ($N_d = 1024$) for comparison. During the phase of ongoing spiral deformation of the disk, the tail of the spiral thins. At low grid resolutions, its thickness falls short of the minimum thickness under which different sides of the spiral begin to influence each other during the interface reconstruction. This leads to numerical breakup during the deformation which subsequently affects the final form of the disk at $\bar{t} = 1$. When the grid resolution is refined, the amount of breakups decreases till they finally no longer occur.
In order to evaluate the quality of the object under investigation (for example the advection scheme or the interface reconstruction method), the deviation of the interface at $\bar{t} > 0$ to its initial position at $\bar{t} = 0$ is quantified by means of an error norm. In this study, we use the L_1 norm in a discrete form, which is defined as

$$L_1(\bar{t}) = \sum_{i,j,k}^{N_d} \left| f(\bar{t})_{i,j,k} - f(0)_{i,j,k} \right| \Delta V_{i,j,k}, \tag{11}$$

Other error norms for evaluating passive advection tests can be found e.g. in [13]. Figure 3a shows the temporal development of the L_1 error with a close-up at around $\bar{t} = 1$ for $N_d = 64$ and for several $a \in [0.1,1]$. In order to highlight the effect of the proposed methodology, the results are compared with results when a standard temporal discretization scheme (explicit Euler method) is used for the passive advection. As can be seen, the minimum error $L_{1,min}$ decreases when a increases for both approaches due to the fact, that $L_{1,min}$ is proportional to the total amount of interface reconstructions [8]. The use of the explicit Euler scheme leads additionally to a temporal shift of $L_{1,min}$ due to the transition error inherent to a temporal discretization scheme. Note that for higher order schemes the temporal shift will be smaller.

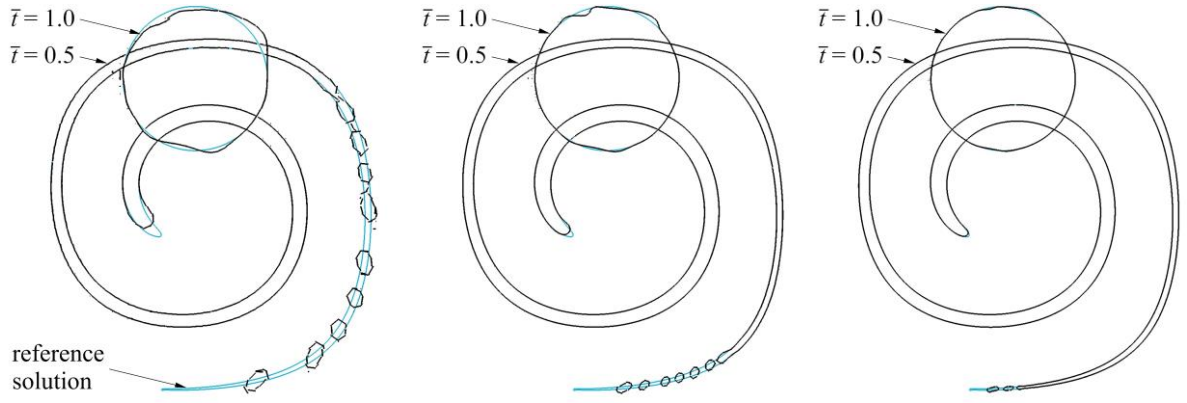

(a) $N_d = 64$ (b) $N_d = 128$ (c) $N_d = 256$

Figure 2. Reconstructed interface (black) at $\bar{t} = t/T = 0.5$ and $\bar{t} = 1.0$ for the 2D deformation flow test by LeVeque [2] for several grid resolutions in comparison to a reference solution ($N_d = 1024$).

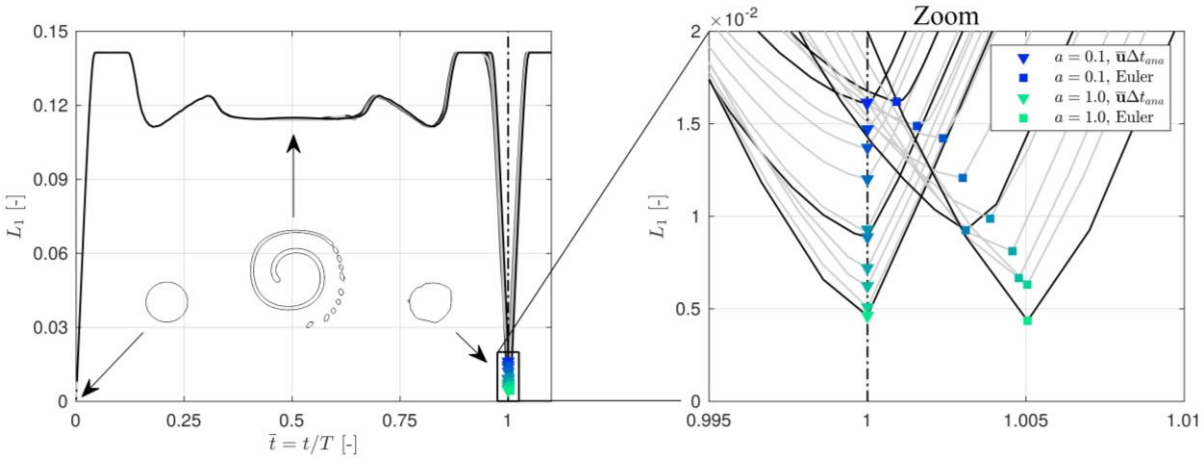

(a)

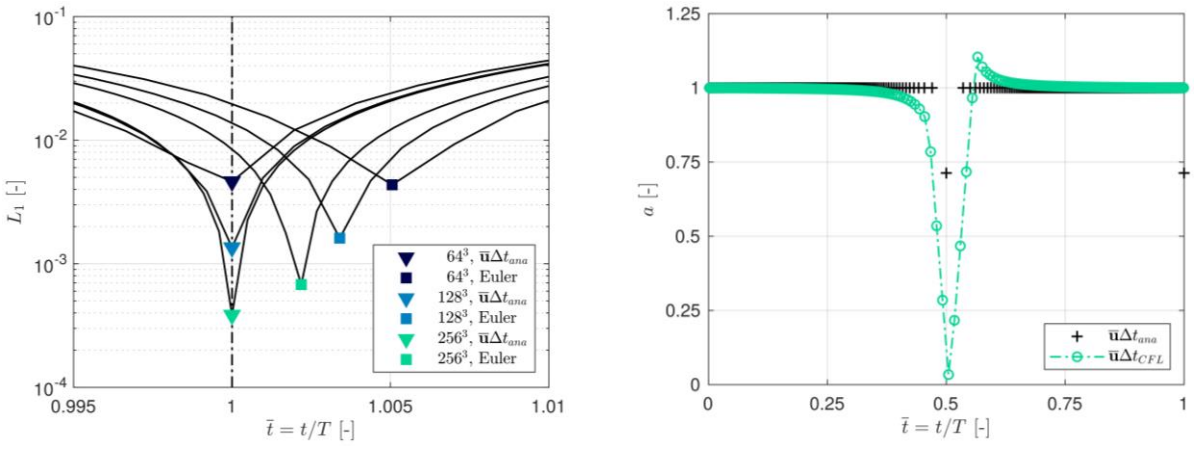

(b) (c)

Figure 3. a) Temporal development of the L_1 error for the 2D deformation flow test with $N_d = 64$ for CFL-numbers a from 0.1 to 1.0 in 0.1 steps. The close up on the right-hand side shows the corresponding minimum errors $L_{1,min}$. The black lines belong to the results with $a \in \{0.1, 0.5, 1.0\}$. b) Temporal evolution of L_1 and $L_{1,min}$ for $N_d = 64$, $N_d = 128$, and $N_d = 256$ for the proposed methodology and when the temporal discretization scheme is used. c) Temporal evolution of the effective CFL-number a for the proposed methodology and when averaged velocities for the flux calculation are used but with the traditional determined time step Δt_{CFL}.

The shift can be decreased by decreasing a, however, at the expense of $L_{1,min}$. Note, that an evaluation of $L_{1,min}$ at $\bar{t} = 1$ would lead to a significant overestimation of the error in this case. In contrast to the used temporal discretization scheme, a temporal shift does not occur in the present case when the proposed methodology is used. The minimum error $L_{1,min}$ is reached at the desired point in time at $\bar{t} = 1$ regardless of the chosen CFL-number a. This is also the case for other grid resolutions as depicted in figure 3b. Nevertheless, it has to be mentioned, that it is not guaranteed that $L_{1,min}$ is exactly reached at $\bar{t} = 1$. In case the advected object disintegrates to a large extent during the advection, further effects like numerical surface tension[2] may affect the overall shape which can lead to a slight temporal shift of $L_{1,min}$. For the sake of completeness, figure 3c shows the temporal development of the effective global CFL-number a when the proposed methodology is used and when averaged velocities with a traditionally calculated Δt_{CFL} by means of the CFL-condition are used for the calculation of F_S. In case the time step is calculated analytically, the CFL-number a remains always constant, except in situations when the velocities or their derivatives change their sign, as discussed above. In contrast to that, the use of Δt_{CFL} leads to a varying a, whereby the deviation from the prescribed a depends only on the rate of change of the given velocity field at the considered point in time. In the present case, this can even lead to an unacceptable violation of the CFL-condition, since situations with $a > 1$ occur.

To facilitate the interpretation of the test results, table 1 shows the obtained errors and results from literature for comparison, which were obtained with various advection schemes and interface reconstruction methods. Besides the L_1 error for various grid resolutions, table 1 shows also the corresponding order of convergence $\mathcal{O}(N_d) = \ln\left(L_1(2N_d)/L_1(N_d)\right)/\ln(1/2)$. Our results show a strong influence of the used test methodology on the test results. The proposed methodology leads to a significant reduction of the L_1 error and to an increase of $\mathcal{O}(N_d)$ with increasing grid resolution in comparison to the case when a standard temporal discretization scheme is used. When the results are compared with data from the literature obtained with a similar advection and interface reconstruction scheme, one can see that FS3D performs well. A general assessment of the accuracy of the used solver in comparison to the other ones remains, however, difficult because only in few of the mentioned studies the used test methodology was described. Without using the same test methodology, a direct comparison can lead to a biased view of the solvers and their advection accuracy. A standardized methodology which excludes influences of temporal discretization schemes would thus help to further improve the comparability between different multiphase solvers.

Table 1 - L_1 errors and corresponding order of convergence $\mathcal{O}$ for 2D deformation flow test with $a = 1$ and $T = 8$.

Method	$L_1(64)$	$\mathcal{O}(64)$	$L_1(128)$	$\mathcal{O}(128)$	$L_1(256)$
RK/Puckett [4]	6.96×10^{-3}	2.27	1.44×10^{-3}	-	-
Stream/Youngs [5]	1.00×10^{-2}	2.22	2.16×10^{-3}	-	-
Hybrid markers-VOF [6]	2.78×10^{-3}	2.54	4.78×10^{-4}	2.04	1.16×10^{-4}
EMFPA/Puckett [7]	6.58×10^{-3}	2.62	1.07×10^{-3}	2.19	2.35×10^{-4}
PCFSC Unsplit/Youngs [8]	7.25×10^{-4}	1.66	2.29×10^{-4}	-	-
Multilevel VOF/ELVIRA [9]	-	-	1.61×10^{-3}	2.46	2.92×10^{-4}
CCU [10]	4.58×10^{-3}	2.20	1.00×10^{-3}	2.59	1.78×10^{-4}
EMFPA-3D [12]	1.04×10^{-2}	2.95	1.34×10^{-3}	1.94	3.49×10^{-4}
UFVFC-Swartz [13]	5.74×10^{-3}	1.98	1.45×10^{-3}	1.95	3.77×10^{-4}
CLSVOF [14]	1.11×10^{-2}	2.48	1.99×10^{-3}	1.93	5.23×10^{-4}
RK3D Split SI/Youngs (Euler)	$\mathbf{4.35 \times 10^{-3}}$	**1.43**	$\mathbf{1.61 \times 10^{-3}}$	**1.25**	$\mathbf{6.79 \times 10^{-4}}$
RK3D Split SI/Youngs $(\bar{u}\Delta t_{ana})$	$\mathbf{4.63 \times 10^{-3}}$	**1.77**	$\mathbf{1.35 \times 10^{-3}}$	**1.81**	$\mathbf{3.85 \times 10^{-4}}$

[2] "Numerical surface tension" in context of multiphase simulations with the VOF-method describes the phenomenon that sharp corners are rounded off due to the stencil-based interface reconstruction, which mimics surface tension.

Conclusions

A methodology for performing passive advection tests for solenoidal and temporal varying velocity fields using the VOF method has been presented. In the proposed methodology the time step for each solution cycle of the advection equation is calculated adaptively and analytically by applying the fundamental theorem of calculus to the underlying time step constraint. The analytical time step Δt_{ana} is then used to calculate exact spatial and temporal averaged velocities for the approximated f-fluxes g_S^n across the faces of the grid cells. The methodology was applied to two very often used passive advection tests and the resulting formulae were given for a rectilinear grid. The methodology can, however, also simply be applied to other time step constraints like e.g. to the one proposed by Weymouth and Yue [18] and it can easily been extended also for unstructured grids. A detailed evaluation of the results for the 2D deformation flow test shows the superiority of the proposed methodology in comparison to the usage of a standard discretization scheme (explicit Euler), where Δt is calculated in a standard way using velocities from t^n. The use of Δt_{ana} leads to a smaller $L_{1,min}$ error and its temporal shift due to the transition error inherent to a temporal discretization scheme vanishes. The biggest advantage is that the results become independent of a temporal discretization scheme since the choice of a, which now remains constant throughout the advection, determines the total number of solution cycles for completing the test. This promotes the comparability of different advection and interface reconstruction schemes and can help to prevent a biased view and misinterpretations of test results in the future.

For arbitrary solenoidal velocity fields it might be, however, not possible to calculate Δt_{ana} in case the time dependence is more complicated. In such a situation, Δt could also be determined semi-analytically by solving the definitions of the CFL-condition with the corresponding averaged velocities at the cell faces iteratively. Furthermore, we assume that an adaption of this methodology to advection schemes in which volume fluxes are not calculated with face averaged velocities should also be possible. This will be, however, investigated in future studies.

Acknowledgement

The authors kindly acknowledge the financial support of the Deutsche Forschungsgemeinschaft (DFG) through the projects SFB-TRR75 (84292822) and EXC 2075 (390740016).

References

[1] Zalesak, S. T., 1979, Journal of Computational Physics 31 (3), pp. 335–362.
[2] Leveque, R. J., 1996, SIAM 33, pp. 627-665.
[3] Rudman, M., 1997, International Journal for Numerical Methods in Fluids 24 (7), pp. 671–691.
[4] Rider, W. J., Kothe, D. B., 1998, Journal of Computational Physics 141 (2), pp. 112–152.
[5] Harvie, D. J. E., Fletcher, D. F., 2000, Journal of Computational Physics 162 (1), pp. 1–32.
[6] Aulisa, E., Manservisi, S., Scardovelli, R., 2003, Journal of Computational Physics 188 (2), pp. 611–639.
[7] López, J., Hernández, J., Gómez, P., Faura, F., 2005, Journal of Computational Physics 208 (1), pp. 51–74.
[8] Liovic, P., Rudman, M., Liow, J.-L., Lakehal, D., Kothe, D., 2006, Computer & fluids 35, pp. 1011–1032.
[9] Cervone, A., Manservisi, S., Scardovelli, R., 2011, Computers & Fluids 47, pp. 101–114.
[10] Comminal, R., Spangenberg, J., Hattel, J. H., 2015, Journal of Computational Physics 283, pp. 582–608.
[11] Roenby, J., Bredmose, H., Jasak, H., 2016, Royal Society Open Science 3, 160405
[12] Owkes, M., Desjardins, O., 2017, Journal of Computational Physics 332, pp. 21–46.
[13] Marić, T., Marschall, H., Bothe, D., 2018, Journal of Computational Physics 371, pp. 967–993.
[14] Wen, H., Yu, C., Sheu, T. W., 2020, Journal of Computational Physics 406, 109188.
[15] Hirt, C. W., Nichols, B. D., 1981, Journal of Computational Physics 39 (1), pp. 201–225
[16] Rieber, M., 2004, Dissertation, Universität Stuttgart.
[17] Youngs, D. L., 1984, Tech. rep., Atomic Weapons Research Establishment AWRE/44/92/35.
[18] Weymouth, G., Yue, D. K.-P., 2010, Journal of Computational Physics 229 (8), pp. 2853–2865.